



Cite this: *RSC Adv.*, 2017, 7, 25597

# Nanostructured fabric with robust superhydrophobicity induced by a thermal hydrophobic ageing process†

Ji-Hyun Oh,<sup>ab</sup> Tae-Jun Ko,<sup>b</sup> Myoung-Woon Moon <sup>\*b</sup> and Chung Hee Park<sup>\*a</sup>

Superhydrophobic surfaces have been fabricated for several applications in clothing, biomedical and engineering fields. However, the durability of the nanostructure itself and the over-coating can be easily damaged during usage by deformation and delamination, respectively. Herein, a robust method to fabricate a superhydrophobic fabric with durable mechanical and chemical properties with a thermally enhanced hydrophobic ageing process is reported. A superhydrophobic PET fabric with a static contact angle of over 160° is fabricated by selective oxygen plasma etching, followed by a heating process, *i.e.* non-chemical finishing. XPS and XRD analysis indicate that a quick hydrophobic ageing occurred due to the reorientation of the PET polymer chains and an increase in newly formed crystallites on the PET surface after the thermal process. Water vapor transmission rate as well as air permeability of the plasma-etched and heated PET fabric sustain similar levels as those of untreated PET fabrics. In addition, the superhydrophobic PET fabric shows strong durability for washing, mechanical robustness and self-cleaning ability even after the surface nanostructures' damage. Thermal hydrophobic ageing process for nanostructured superhydrophobic textiles uses no chemicals for surface finishing, which results in improved wearing comfort and human/environment friendliness, thus attracting attention from the textile or biomedical goods and related industries.

Received 3rd April 2017  
 Accepted 26th April 2017

DOI: 10.1039/c7ra03801a

[rsc.li/rsc-advances](http://rsc.li/rsc-advances)

## Introduction

Superhydrophobic surfaces, exhibiting a static water contact angle of >150°, have been utilized for various different materials such as glass,<sup>1</sup> fabrics,<sup>2,3</sup> metal<sup>4</sup> and sponge<sup>5</sup> for their functional properties, for instance, water-resistance, self-cleaning, and anti-fogging. Superhydrophobic surfaces can be obtained by the combination of two major parameters *i.e.*, surface roughness on the nano- or microscale and low-surface-energy overcoating as the hydrophobic finishing coating.<sup>6</sup> Recently, several studies have reported superhydrophobicity on fabrics formed with inorganic particles such as SiO<sub>2</sub>,<sup>7</sup> TiO<sub>2</sub><sup>8</sup> and ZnO.<sup>9</sup> Addition of nanoparticles on the fabric surfaces does not preserve surface roughness, and consequently the detachment may cause hazardous effects to human health since the nanomaterials have mostly non-covalent bonds that link them to the fabric. Plasma or ion beam-based nanostructuring has been studied as an alternative way to create superhydrophobicity on fabrics,<sup>2,3</sup> wherein after nanostructuring, over-coating with a low-surface-

energy material is introduced since the plasma-treated surface shows hydrophilicity.<sup>10</sup>

Nanostructures formed on fabrics by plasma treatment show some weakening in the structural stability during use or washing because of the damage of the nanostructure itself and the delamination of the low-surface-energy material coating, which results in a decrease in the superhydrophobicity. Consequently, this additional coating limits the application of the nanostructured superhydrophobic fabric, particularly in clothing. For materials with low surface energy, academic and industrial fields have greatly used chemicals containing fluorine compounds because of its good water resistance, but they are costly.<sup>11</sup> However, fluorine compounds released during manufacturing, use or disposal are harmful to human health and the environment. Hence, reduced usage of fluorine compounds and development of alternative methods are required.<sup>12</sup> Some researchers reported that hydrophobic surfaces can be obtained using non-fluorine compounds such as PDMS (polydimethylsiloxane) for dip-coating,<sup>13</sup> lauryl methacrylate for spraying method<sup>14</sup> or HMDSO (hexamethyldisiloxane) for plasma treatment.<sup>15</sup> Moreover, the fabrics made by dip-coating and spraying method<sup>14,16</sup> are covered with solutions that fill the pores of the fabric. As a result, the fabrics show a decline in unique properties, for instance flexibility or breathability, a major factor in regulation of the thermo-physiological comfort of the human body.<sup>17</sup> Moreover, the surface coated with hydrophobic plasma shows damages like

<sup>a</sup>Department of Textiles, Merchandising and Fashion Design, Seoul National University, Seoul, 08826, Republic of Korea. E-mail: junghee@snu.ac.kr

<sup>b</sup>Materials and Life Science Research Division, Korea Institute of Science and Technology, Seoul, 02792, Republic of Korea. E-mail: mwmoon@kist.re.kr

† Electronic supplementary information (ESI) available. See DOI: 10.1039/c7ra03801a



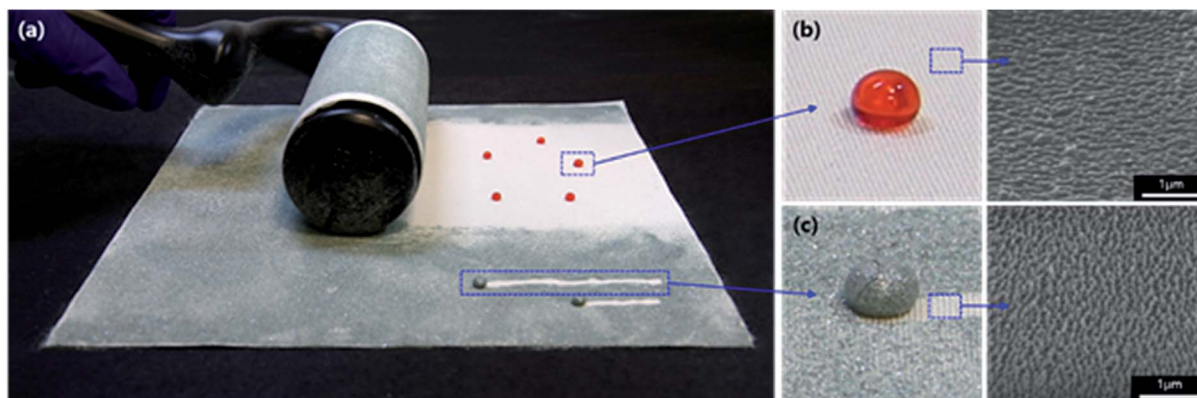


Fig. 1 Photographs of the PET fabric plasma-etched for 60 min and heated at 130 °C for 24 h after scattering silicon carbide particles on the surface (a) and cleaning with a commercial daily household clothing roll tape cleaner (b) and water droplets (c).

cracks or delamination of the coated materials caused by water, which means that hydrophobic plasma-coated surfaces have low durability.<sup>18</sup>

In this study, we proposed an effective but simple method to fabricate robust nanostructured superhydrophobic PET (polyethylene terephthalate) fabrics formed using only heating treatment. The fabric surface becomes hydrophilic when plasma-etching is carried out *via* an oxygen plasma treatment. With time, the plasma-etched surface shows ageing behaviour, reverting to the original hydrophobic state of the PET material.<sup>19</sup> However, the recovery rate from hydrophilic to superhydrophobic is slow with time and pressure, whereas it can be significantly enhanced through the thermal treatment process.<sup>20</sup> Accordingly, the fabrics nanostructured by plasma-based selective etching and by thermal treatment show a robust superhydrophobicity because of the surface roughness and hydrophobic recovery, respectively.<sup>21</sup> Superhydrophobicity of the developed fabric was evaluated by measuring the static contact angles and shedding angles. Chemical composition, surface modification and crystallinity were examined using XPS, SEM and XRD. The levels of breathability were decided based on the water vapor transmission rate (WVTR) and air permeability. As for the durability tests, tape and pressure tests were conducted to determine whether the plasma-etched and heated superhydrophobic PET fabric can bear physical impact, as shown in Fig. 1.

## Experimental

### Material and surface modification

The fabric was 100% PET consisting of a yarn count of 75d/72f + 150d/144f DTY (Draw Textured Yarn) and weave density of 144 × 80 (in inch), and the weight ( $\text{g m}^{-2}$ ) and thickness (mm) were 108 and 0.21, respectively. The largest specimen size was 25 cm × 25 cm. Oxygen plasma was utilized to make the nanostructured surface. The plasma power and substrate bias voltage were 238 W and -400 V, respectively. The oxygen gas flow rate was set at 50 sccm and the durations were 0, 5, 15, 30 and 60 min. Surface roughness change was observed by scanning electron microscopy (SEM, Nova NanoSEM 200, FEI, USA).

A 10 nm thick Pt film was covered onto the fabric to provide better conductivity and prevent the generation of electron charge. The SEM electron accelerating voltage was 10 kV, and chemical composition change was analyzed using X-ray photoelectron spectroscopy (XPS, PHI 5000 Versa Probe (Ulvac-PHI), USA) with 24.5 W and 15 kV. XRD patterns were obtained using a Dmax2500/PC (Rigaku) at 40 kV and 200 mA and Cu-K $\alpha$  radiation ( $\lambda = 1.5406 \text{ \AA}$ ). The  $2\theta$  angle used was from 10° to 50° and the scan speed and scan width were 2° min<sup>-1</sup> and 0.02°, respectively.

### Thermal hydrophobic ageing process

Water contact angles of the fabrics that were plasma-etched for various durations (0, 5, 15, 30 and 60 min) and heated at high temperatures (130 °C and 180 °C) for 0, 1, 3, 9, 15 and 24 h were measured on both sides of the fabrics. A contact angle goniometer (Theta Lite, Attension, Finland) was used, and the dropped deionized (DI) water had a volume of  $4.0 \pm 0.5 \mu\text{L}$ . The shedding angle developed by Jan Zimmermann was assessed using the same equipment used for the static contact angle measurement.<sup>22</sup> The distance between the syringe tip and the sample surface was fixed at 10 mm. A water droplet with a volume of  $12.5 \pm 0.1 \mu\text{L}$  was dropped, and the angle was measured when rolling off over 2 cm. We also conducted water droplet impact test to simulate the water resistance of the surfaces to a raindrop. The height from the syringe tip to the PET fabric was 70 mm. The bouncing moves on both PET fabrics, untreated, and plasma-etched for 60 min and heated at 130 °C for 24 h, were recorded with a high-speed motion camera (FASTCAM Mini UX50, Photon, Marlow, UK).

### Suitability of clothing: water vapor transmission rate (WVTR), air permeability, tensile strength and color change

The wearing comfort can be assessed using the water vapor transmission rate (WVTR), using ASTM E96-80. A fabric with a diameter of 7 cm was placed on a water vapor permeability cup, which was pre-heated to a temperature of  $40 \pm 2 \text{ °C}$  and then filled with 33 g of anhydrous calcium chloride (SHOWA). The cups were placed in a conditioned chamber at  $40 \pm 2 \text{ °C}$  and



relative humidity (RH) of  $90 \pm 5\%$  for 1 hour and then weighed. The measured cups were put into the conditioning chamber for another hour and measured for weight changes. The average weight change of three replicates was calculated. Air permeability, representing the passing volume of air through the fabric, was tested by ASTM D737-7515 with an air permeability tester (FX3300, TEXTEST, Switzerland). The 5 different fabrics conditioned at  $20 \pm 2^\circ\text{C}$  and  $65\% \pm 5\%$  RH for 24 hours were tested at a pressure of 125 Pa. Tensile strength was tested using a Universal Testing Machine (Instron-5543, Instron, USA) according to the ASTM D 5035 strip method, and color change test was performed using a color-difference meter (CM-2600d, Minolta, Japan).

### Durability test: tape test, self-cleaning test after rolling commercial tape cleaner, pressure test, washing durability and pH test

The tape test was performed according to ASTM D3359 with a Scotch Tape (3M, 810) and a commercial roll tape cleaner for clothing. The tape of 25 mm width was attached on the plasma-etched and heated superhydrophobic PET fabric and then rubbed gently with an eraser on the end of a pencil. After rubbing 5 or 10 times, static contact angles and shedding angles of the tested fabrics were measured. Furthermore, the commercial tape cleaner was rolled several times on the contaminated surface to perform a thorough cleaning, which presents a practical test of the self-cleaning effect. For the pressure test, weights of 900 and 1800 g (a diameter of 57 mm and height of 35 mm) were placed on the plasma-etched and heated superhydrophobic PET fabric for 10 min. Subsequently, static contact angles were evaluated. These procedures were repeated three times. The washing durability of the plasma-etched and heated superhydrophobic PET fabrics was determined under aqueous washing. For aqueous washing, tap water was used at  $20^\circ\text{C}$  in a liquid ratio of 1 : 200 without detergent and agitating with a magnetic stirrer at 300 rpm for 10 min. After washing, specimens were dried at room temperature ( $24^\circ\text{C}$ , 22%) for 1 day. An extra heating process at  $130^\circ\text{C}$  for 1 hour was conducted to determine whether the decreased static contact angle during the washing test could be increased. The average of the static contact angles and the shedding angles at 9 different spots in each of the 3 specimens were recorded. For the pH test, the pH of the solutions was varied from 7 to 1 by adding hydrochloric acid (HCl) and from 7 to 11 by adding sodium hydroxide (NaOH) to DI water. The plasma-etched and heated PET fabrics were dipped and stirred at 400 rpm in the solutions for 30 min, rinsed with water and dried at room temperature.

### Self-cleaning test

In order to measure the self-cleaning property, silicon carbide particles as contaminants, were scattered on the plasma-etched and heated superhydrophobic PET fabric tilted at  $10^\circ$ , and the contaminants were subsequently removed by application of distilled water droplets.

## Results and discussion

### Surface modification

The mechanism of thermal hydrophobic recovery is presented in Fig. 2a. The surface of the plasma-etched PET fabric had free radicals or polar groups generated from oxygen plasma. In order to minimize the surface energy of the plasma-etched surface, plasma-induced polar groups diffuse into the polymer, leading the non-polar groups to move to the surface.<sup>21</sup> Consequently, the plasma-etched and heated PET fabric with a high aspect ratio surface roughness would recover hydrophobicity. Usually this recovery rate is slow with time and can be accelerated by applying a thermal process.<sup>20</sup>

PET fabrics after plasma etching were examined by SEM, as shown in Fig. 2b, c, e, f, h and i. After the heating process, no significant change in the topology was found on the nano-structured fabrics (Fig. 2f and i). In addition, a bump-like structure was observed on the surfaces as shown in Fig. 2h and S1,† which was verified as a part of the PET fabric (Fig. S2†) and the newly increased crystallinity (Fig. S3†). On the other hand, the static contact angles increased from superhydrophilicity to superhydrophobicity as presented in Fig. 2g and j. When dropped several times, water droplets did not attach and rolled right off after being dropped on the PET fabric

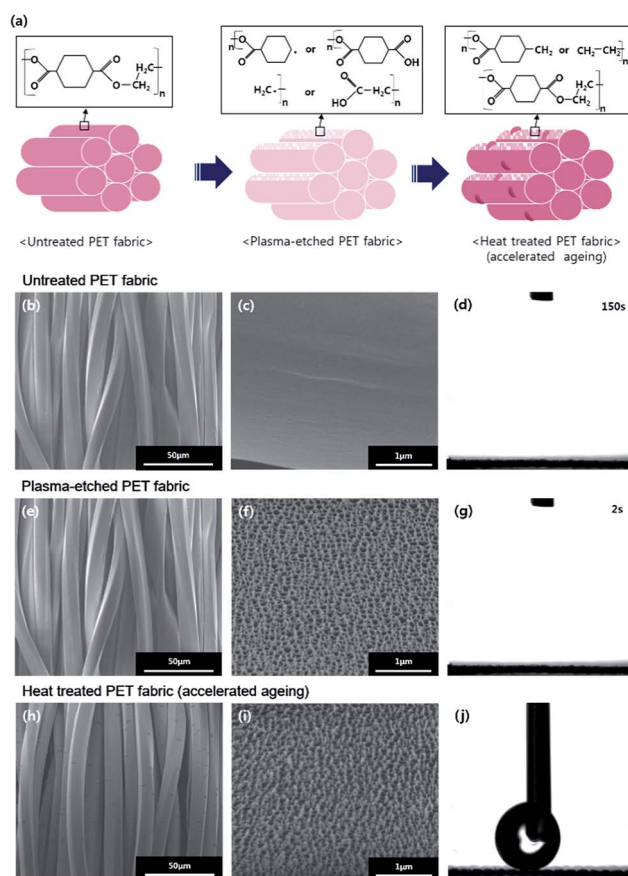


Fig. 2 Schematic (a), SEM images and static contact angle change for untreated (b–d), 60 min plasma-etched (e–g) and 60 min plasma-etched and heated at  $130^\circ\text{C}$  for 24 h (h–j) PET fabrics.



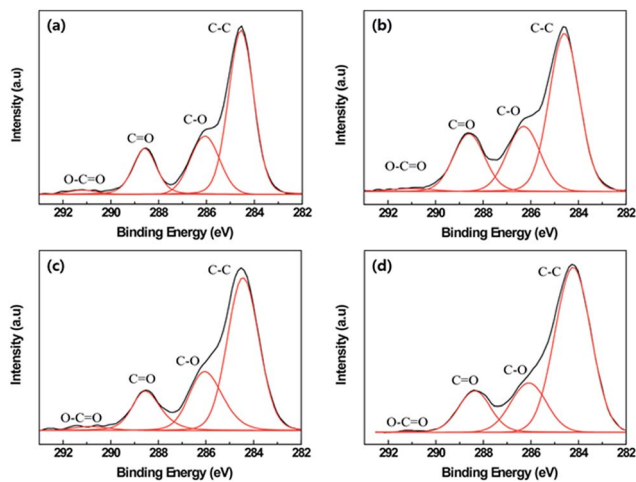


Fig. 3 XPS survey spectra for PET fabrics untreated (a), plasma-etched for 60 min (60E) (b), heated at 130 °C for 24 h (130 °C) (c) and plasma-etched for 60 min and heated at 130 °C for 24 h (60E + 130 °C) (d).

that was plasma-etched for 60 min and heated at 130 °C for 24 h. However, we tried to measure the water contact angles as carefully as possible, and the static contact angle of water was more than 174°.

It was determined that the chemical composition of the PET fabrics changed on plasma etching.<sup>21</sup> Fig. 3 shows the XPS C1s spectra for 4 cases of the PET fabrics: untreated, plasma-etched for 60 min, heated at 130 °C for 24 h and plasma-etched for 60 min and heated at 130 °C for 24 h. Four separate peaks at 284.61, 286.33, 288.61 and 290.99 eV, corresponding to the C–C group, C–O group, C=O group and O–C=O group, were detected. The untreated PET fabric had C–C, C–O, C=O and O–C=O groups of about 58.71%, 23.18%, 16.48% and 1.65%, respectively. With increasing the oxygen plasma etching time up to 60 min, C–C groups decreased to 54.14%, whereas C–O and C=O groups increased. This phenomenon was confirmed using elemental composition analysis (Table 1). Carbon content decreased by 16.48%, but oxygen content increased by 16.48%. These results verified that polar groups containing oxygen groups were induced on the surface of the PET fabric by oxygen plasma etching. As the PET fabric plasma-etched for 60 min was subsequently heated at 130 °C for 24 h, the chemical composition was changed because of the increase in the carbon content and a decrease in the oxygen content. The C–C group

displayed the highest value of 65.01% among all the specimens, and the values of the other groups decreased. This is because the 60 min plasma-etched PET fabrics having many polar groups on the surface tended to minimize the surface energy and returned to the equilibrium state for polymer chain re-orientation. The surface free energies of the PET untreated, plasma-etched for 60 min and air can be defined as  $\gamma_u$ ,  $\gamma_p$  and  $\gamma_a$ , respectively. Therefore, it can be assumed that their order is  $\gamma_p > \gamma_u > \gamma_a$ , because PET fabrics untreated and plasma-etched for 60 min absorbed a water droplet at 150 s and 2 s, respectively (Fig. 4b and c). Therefore, as the relationship of the interface free energy between the 60 min plasma-etched PET fabric and air, and untreated fabric and air is satisfied with  $(\sqrt{\gamma_p} - \sqrt{\gamma_a})^2 > (\sqrt{\gamma_u} - \sqrt{\gamma_a})^2$ , and it is known that the contact of air with the untreated PET fabric is thermodynamically favorable.<sup>23</sup> Consequently, the 60 min plasma-etched PET fabric spontaneously decreased the free energy of the interface by diffusion of the polar groups induced during the oxygen plasma treatment inside of the PET fabric. The heating process accelerates the migration of polar groups into the fabric,<sup>24</sup> which results in a quick hydrophobic recovery on the 60 min plasma-etched PET fabric.

### Surface hydrophobicity

Water repellency of the PET fabrics was evaluated using static contact angles (Fig. 4). The untreated PET fabric had a zero degree static contact angle, indicating absorption of the water droplet in 150 s; however, the PET fabric plasma-etched with oxygen plasma for 60 min was superhydrophilic, with the water droplet permeating in 2 s (Fig. 4b and c). The PET fabric untreated or plasma-etched, followed by keeping those samples at room temperature were hydrophilic regardless of the durations of plasma etching (Fig. 4a). However, the fabrics that were plasma-etched for 60 min and heated at 130 °C for 24 h and those that were plasma-etched for 30 or 60 min and heated at 180 °C for 24 h showed superhydrophobicity. As shown in Fig. 4d, when the water droplets were dropped on the plasma-etched and heated PET fabric, they were not absorbed or attached on the surface, showing a static contact angle of  $174^\circ \pm 1.2^\circ$ . This result originated from the hierarchical surface roughness and recovered hydrophobicity of the PET material. At a heating temperature of 130 °C, the surface was superhydrophobic at a plasma etching time of 60 min, while at the

Table 1 Concentration of the different carbon groups and surface elemental composition of PET fabrics untreated (a), plasma-etched for 60 min (60E) (b), heated at 130 °C for 24 h (130 °C) (c) and plasma-etched for 60 min and heated at 130 °C for 24 h (60E + 130 °C) (d)

	Bonding contribution (At%)				Elemental composition (At%)	
	C–C at 284.61 eV	C–O at 286.33 eV	C=O at 288.61 eV	O–C=O at 290.99 eV	C	O
(a) Untreated PET	58.71	23.18	16.48	1.65	73.76	26.24
(b) 60E PET	54.14	23.81	20.58	1.47	57.28	42.72
(c) 130 °C PET	57.84	21.78	15.22	1.82	70.74	29.26
(d) 60E + 130 °C PET	65.01	19.4	15.37	0.23	61.38	38.62



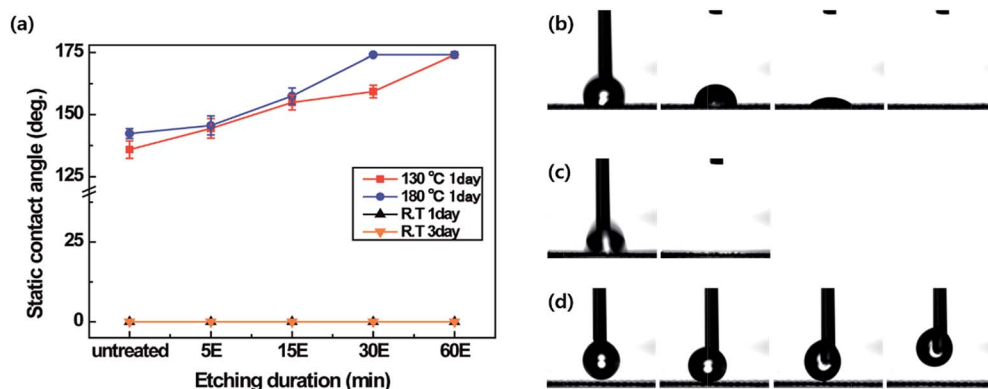


Fig. 4 Graph of static contact angles depending on various etching durations and ageing temperatures (a) and bouncing images of water droplets on the surface of untreated PET fabric (b), plasma-etched for 60 min PET fabric (c) and plasma-etched for 60 min and heated at 130 °C for 24 h PET fabric (d).

heating temperature of 180 °C, superhydrophobicity was observed at a shorter plasma etching time of 30 min. This is because the hydrophobic ageing process is accelerated with increasing heating temperatures, that is to say, the high temperature expedites polymer chain reorientation. The optimum condition for the superhydrophobic PET fabric was plasma etching for 60 min and heating at 130 °C since temperatures of 105 °C or less did not affect the hydrophobic recovery of the fabrics (Fig. S4†). Note that plasma etching-based nanostructuring, followed by hydrophobic coatings with HMDSO<sup>2</sup> or CF<sub>4</sub> and C<sub>2</sub>H<sub>2</sub><sup>3</sup> require shorter etching times to show superhydrophobicity compared to the results obtained from this study. The overcoating chemicals may have lower surface energy than that for the recovered surface of heated PET by the heating process.<sup>21</sup>

Changes in the water contact angle were determined based on the ageing durations (0, 1, 3, 6, 9, 15 and 24 h) (Fig. 5). Even though the untreated PET fabric absorbed a water droplet

within 150 s, the PET fabric plasma-etched for 60 min soaked a water droplet immediately because of the high-aspect ratio nanostructures and the polar groups induced during oxygen plasma etching. After heating, particularly for 3 h, the static contact angles of the untreated PET fabric increased, which might be caused by hydrophobic thermal ageing as discussed above. The PET fabric plasma-etched for 60 min showed hydrophobicity according to the heating time, and at the end of 24 h it showed superhydrophobicity due to the high aspect ratio nanostructures and hydrophobic thermal recovery. In addition, the PET fabric plasma etched for 60 min and heated at 130 °C for 24 h maintained its high static contact angles for liquids having surface energy of from 72.8 up to 50 dyne cm<sup>-1</sup> (Fig. S5†). However, the fabric plasma-etched for 60 min without any heat treatment showed superhydrophilicity up to approximately 1 month since hydrophobic recovery is slow with time.

The water impacting experiment was performed to simulate the resistance of a raindrop on the fabrics untreated and plasma-etched for 60 min and heated at 130 °C for 24 h as shown in Fig. 6. It was observed that a water droplet was pinned and absorbed on the untreated PET fabric surface without any bouncing (Fig. 6a). On the contrary, a water droplet gently bounced on the plasma-etched and heated fabric, leaving no residue of water (Fig. 6b), indicating the high robustness in water repellency. Therefore, it can be considered that the

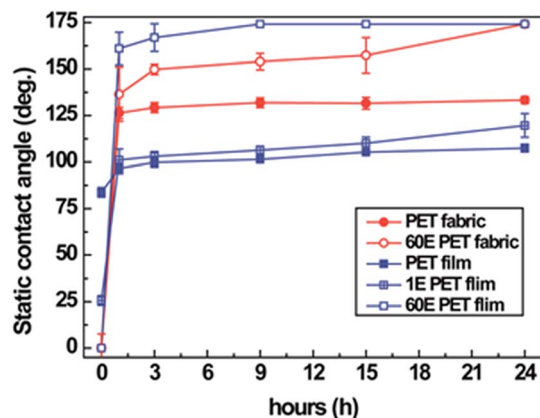


Fig. 5 Effect of thermal ageing time on the contact angles of water drops on PET films or fabrics; untreated PET fabric (filled red circle), PET fabric plasma-etched for 60 min and heated at 130 °C (empty red circle) and untreated PET film (filled square), PET film plasma-etched for 1 min (1E, square filled with cross) and PET film plasma-etched for 60 min and heated at 130 °C (empty square).

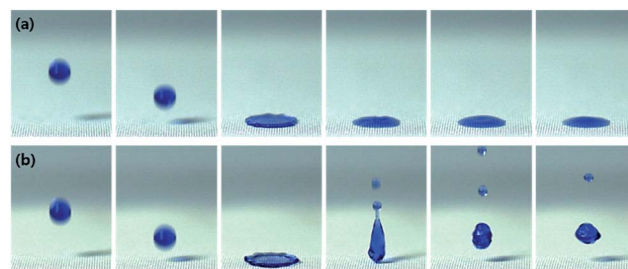


Fig. 6 Bouncing behavior of water droplets on the PET fabrics untreated (a) and plasma-etched for 60 min and heated at 130 °C for 24 h (b).



superhydrophobic fabric can be strongly resistant to water impact, better than the untreated fabric.

### Suitability of clothing

Good breathability of clothing involves maintaining the inside of the clothing dry and comfortable by diffusing the sweat generated by human body to the exterior of the fabric. Water vapor transmission and air permeability are important parameters to assess this breathability of clothing.<sup>25</sup> The superhydrophobic PET fabrics plasma-etched for 60 min and heated at 130 °C for 24 h transmitted water vapor efficiently to the outside, showing a similar water vapor transmission rate (WVTR) as that of the untreated PET fabric (Fig. 7). This feature might originate from the asymmetric surface of the superhydrophobic PET fabric in which the bottom side of fabric showed hydrophilicity and absorbed water in 40 min, while the top side of the fabric exhibited superhydrophobicity<sup>2,26</sup> (Fig. S6†). Moreover, under the high temperature heating process, PET fabrics shrank because of disorientation in the oriented amorphous regions or chain folding.<sup>27</sup> The contracted PET fabrics might have less air permeability, leading to low breathability. As another important factor that reflects breathability, air permeability changes of PET fabrics were evaluated. As seen in Fig. 7, the amount of air permeability was not diminished after the etching process and exhibited a very minor decrease after the heating process, which implies that there was not a significant contraction of the PET fabric because of the heating process. Moreover, when the PET fabric was plasma-etched and then heated, air permeability showed a slight decrease, but its value was within the margin of error of the air permeability of untreated PET fabrics, showing the decrease by  $0.52 \text{ cm}^3 \text{ s}^{-1} \text{ cm}^{-2}$ . This result suggested that the heating process within 130 °C does not cause high contraction of PET fabrics, and thus does not significantly affect the porosity of the PET fabrics. Therefore, based on water vapor transmission and air permeability, the plasma-etched and heated superhydrophobic PET fabric represents good breathability. Furthermore, even though the PET fabric underwent plasma etching or heating process, the tensile strength of the PET

fabrics was not significantly changed (Fig. S7†). In addition, the color change of the PET fabric before and after plasma etching or heating process was also investigated as shown in Fig. S8.† It was found that, compared to the color of the untreated PET fabric, the heated PET fabric had a slightly yellow color, and the etched PET fabric had a yellowish and dark color. Therefore, when plasma-etched and heated, PET fabric had more yellowish and darker color, compared to the untreated PET fabric (Fig. S8†). It might be considered that the heating temperature above  $T_g$  of the PET fabric and the reflection of the incident light by the nanostructures on the fabrics can cause a change in color on the plasma-etched or heated fabric. However, this cannot be the case if the fabric is dyed.

### Durability test

The low mechanical durability of the nanostructures is the limiting factor for the use or wear of superhydrophobic fabric because nanostructures are easily damaged by external contact like pressure or power. In order to test the durability of the plasma-etched and heated PET fabric, tape, weight and washing tests were conducted. ASTM tape test results showed that the superhydrophobicity decreased because the stickiness of the scotch tape 810D indicated that the standard test caused the fabric to wear out (Fig. S9 and S10†). So, the tape test was followed by a modified ASTM tape test that used a commercial daily household clothing roll tape cleaner. The results showed that despite the little damage to the superhydrophobic PET fabrics, the surface was clean without any visible sticky substances and the surface roughness was maintained (Fig. 1b and 8a–d). Superhydrophobicity was maintained even after the rolling tape cleaner test was repeated 5 and 10 times (in case of 50 trials-average:  $144.6^\circ$ , deviation:  $5.8^\circ$ ). As shown in Fig. 1, after completely eliminating the silicon carbide particles on the superhydrophobic PET fabric with repeated rolling of the tape cleaner, the water droplets dyed with red ink were formed as spheres and were not absorbed onto the superhydrophobic PET fabrics. Washing durability was also tested under mild washing conditions using tap water. As shown in Fig. 8e, the superhydrophobicity gradually decreased by water washing, though not significantly. Fig. S11† indicated that the decrease in the superhydrophobicity might be caused from the bended nanostructures that are deformed by centrifugal force during agitation, which induces a low surface roughness and decreases the superhydrophobicity. Furthermore, another possibility is that upon repeated washings, the surface molecular rearrangement might occur in a way for hydrophilic groups to face water because water induces molecular rearrangement and thus the surface hydrophobicity decreases by washing.<sup>28</sup> However, the decreased superhydrophobicity was improved by an additional heating process at 130 °C for 1 h and resulted in a static contact angle of over  $160^\circ$  and shedding angle of below  $10^\circ$ . Thus, the contaminated superhydrophobic PET fabric developed by etching and heating could be washed with water and used in daily life. In addition to the mechanical robustness, we also checked the chemical durability using solutions with various pH 1, 3, 5, 7, 9 and 11. As shown in Fig. 9, it was found that there

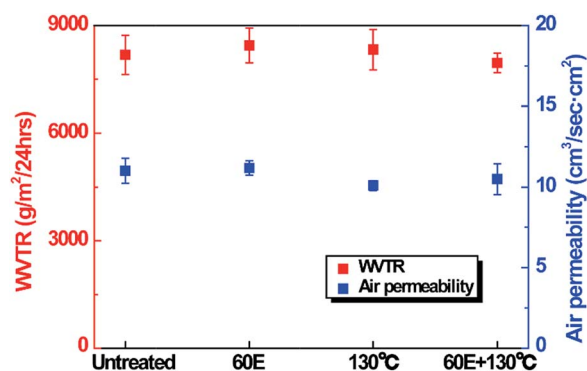


Fig. 7 Water vapor transmission rate (WVTR) and air permeability of untreated, plasma-etched for 60 min PET fabric, heated at 130 °C for 24 h PET fabric and plasma-etched for 60 min and heated at 130 °C for 24 h PET fabric.



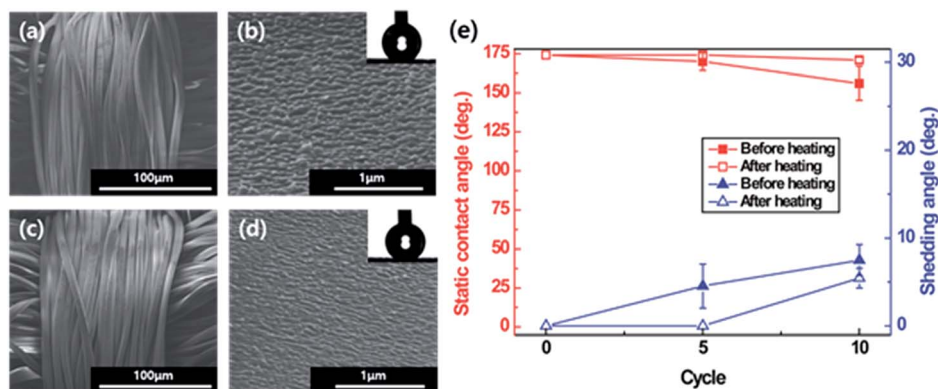


Fig. 8 SEM images of plasma-etched for 60 min and heated at 130 °C for 24 h PET fabrics after tape test with commercial daily household clothing roll tape cleaner: 5 times (a and b) and 10 times (c and d) and effect of heating on the static contact angles and shedding angles of repeatedly washed PET fabrics plasma-etched for 60 min and heated at 130 °C for 24 h (e).

are no changes in the static contact angles for solutions of pH 3, 5, 7 and 9 since the surface materials are the same and the nanostructures are chemically inert before and after plasma treatment. However, in the solutions of pH 1 and 11, the static contact angles relatively decreased to 165.84° and 163.63°, respectively. This might be because the PET fabric was slightly degraded in strong acid and alkaline solutions even though it had good chemical resistance. Moreover, they showed self-healing, having a contact angle of 174° ± 1.2° after heating at 130 °C for 60 min and 90 min, respectively. From these results,

it can be concluded that even after some damage occurred mechanically or chemically, superhydrophobicity would be recovered by the heating process.

### Self-cleaning test

Because of the self-cleaning property, superhydrophobic fabrics can maintain dirt-free conditions and reduce the number of washing cycles, which leads to efficient management of the superhydrophobic fabrics. Hence, self-cleaning test was performed. Contaminants, silicone carbides, were eliminated perfectly along a path of rolling water droplets, illustrating the self-cleaning property<sup>29</sup> as shown in Fig. 1c. Moreover, a large sized specimen of 25 cm × 25 cm was used for the self-cleaning test, indicative of the adaptability of plasma etching and heating process to large-scale specimens. Silicon carbide particles were spread on the plasma-etched and heated PET fabric tilted at 10° (Fig. 10). Right after dropping distilled water droplets, the pollutants were removed, followed by the water droplets. The distance that water droplets rolled down was much longer than 2 cm, approximately 20 cm (Fig. 10). The water droplets stopped rolling when they were saturated with silicon carbide particles. This result showed that the superhydrophobic PET fabric developed by etching and ageing has excellent self-cleaning property, even in the large-scaled specimen, which suggested that the superhydrophobic fabric developed in this study would be utilized and commercialized for the clothing industry.

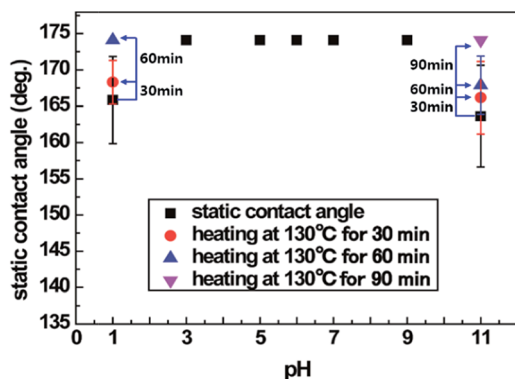


Fig. 9 Static contact angle change of plasma-etched for 60 min and heated at 130 °C for 24 h PET fabric after exposure to liquids with various pH solutions.

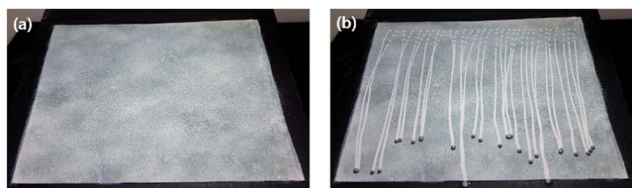


Fig. 10 Self-cleaning photographs of PET fabric plasma-etched for 60 min and heated at 130 °C for 24 h contaminated with silicon carbide particles before (a) and after dropping water droplets (b).

## Conclusions

Superhydrophobic PET fabric was achieved using selective etching by oxygen plasma and heating process without finishing coating. The PET fabric was nanostructured by plasma etching for 60 min to create hierarchical structures on the surface, and the heating process at 130 °C for 24 h was found to accelerate the hydrophobic ageing effect, leading to a conversion of the property from hydrophilicity to superhydrophobicity. The plasma-etched and heated superhydrophobic PET fabric exhibited good water repellency, maintaining high contact angle for the various liquids having a surface tension of 50 dyne cm<sup>-1</sup>. Breathability



(water vapor transmission rate and air permeability) and tensile strength of the superhydrophobic PET fabric were kept at the level of that of the untreated PET and showed good characteristics. However, the color of the superhydrophobic PET fabric became yellowish and darker for the case of plasma etching and heating, but this will not matter if the fabric is dyed. Furthermore, the superhydrophobicity was sustained after applying the pressure test with weights of 900 and 1800 g (Fig. S12†). The fabric showed good durability with the tape test with a commercial rolling tape, washing test with a water solution and pH test with various pH solutions, although some of the nanostructures were damaged. The self-cleaning property of the superhydrophobic PET fabric was also excellent. These results indicated that the plasma-etched and heated PET fabric has robust nanostructure durability with regard to the mechanical and chemical treatment. Thus, the nanostructured superhydrophobic PET fabric fabricated by the non-chemical finishing method can be widely employed in indoor or outdoor clothing and biomedical goods etc.

## Acknowledgements

This study was supported by a KIST internal project. The authors also acknowledge support from the Center for Advanced Materials (CAMM) funded by the Ministry of Science, ICT and Future Planning as Global Frontier Project (CAMM-No. 2014063701) as well as a grant [MPSS-CG-2016-02] through the Disaster and Safety Management Institute funded by Ministry of Public Safety and Security of Korean government. This work was also supported by a grant (no. 2015R1A2A2A03002760) of the National Research Foundation (NRF) of Korea funded by the Korean government (MSIP) and by the BK21 Plus Project (grant no. 22B20130000043) of the NRF of Korea grant funded by the Korean government.

## References

- 1 E. Yu, S. C. Kim, H. J. Lee, K. H. Oh and M. W. Moon, *Sci. Rep.*, 2015, **5**, 9362.
- 2 S.-o. Kwon, J. Kim, M.-W. Moon and C. H. Park, *Text. Res. J.*, 2016, **87**, 807–815.
- 3 J.-H. Oh, T.-J. Ko, M.-W. Moon and C. H. Park, *RSC Adv.*, 2014, **4**, 38966.
- 4 J. T. Han, Y. Jang, D. Y. Lee, J. H. Park, S.-H. Song, D.-Y. Ban and K. Cho, *J. Mater. Chem.*, 2005, **15**, 3089.
- 5 Q. Zhu, Y. Chu, Z. Wang, N. Chen, L. Lin, F. Liu and Q. Pan, *J. Mater. Chem. A*, 2013, **1**, 5386.
- 6 X. Deng, L. Mammen, H.-J. Butt and D. Vollmer, *Science*, 2012, **335**, 67–70.

- 7 Q. An, W. Xu, L. Hao, Y. Fu and L. Huang, *J. Appl. Polym. Sci.*, 2013, **128**, 3050–3056.
- 8 Y. Shi, Y. Wang, X. Feng, G. Yue and W. Yang, *Appl. Surf. Sci.*, 2012, **258**, 8134–8138.
- 9 M. Zhang, C. Wang, S. Wang and J. Li, *Carbohydr. Polym.*, 2013, **97**, 59–64.
- 10 J. Lai, B. Sunderland, J. Xue, S. Yan, W. Zhao, M. Folkard, B. D. Michael and Y. Wang, *Appl. Surf. Sci.*, 2006, **252**, 3375–3379.
- 11 B. Mahltig, H. Haufe and H. Böttcher, *J. Mater. Chem.*, 2005, **15**, 4385.
- 12 S. Hoshian, V. Jokinen, V. Somerkivi, A. R. Lokanathan and S. Franssila, *ACS Appl. Mater. Interfaces*, 2015, **7**, 941–949.
- 13 H. F. Hoefnagels, D. Wu, G. d. With and W. Ming, *Langmuir*, 2007, **23**, 13158–13163.
- 14 L. Wang, X. D. Liu, G. H. Xi, S. J. Wan and C. H. Zhao, *Cellulose*, 2014, **21**, 2983–2994.
- 15 B. Shin, K.-R. Lee, M.-W. Moon and H.-Y. Kim, *Soft Matter*, 2012, **8**, 1817–1823.
- 16 K. Sasaki, M. Tenjimbayashi, K. Manabe and S. Shiratori, *ACS Appl. Mater. Interfaces*, 2016, **8**, 651–659.
- 17 H. N. Yoon and A. Buckley, *Text. Res. J.*, 1984, **54**, 289–298.
- 18 H. Yasuda, Q. S. Yu and M. Chen, *Prog. Org. Coat.*, 2001, **41**, 273–279.
- 19 C. Borcia, I. L. Punga and G. Borcia, *Appl. Surf. Sci.*, 2014, **317**, 103–110.
- 20 N. De Geyter, R. Morent and C. Leys, *Nucl. Instrum. Methods Phys. Res., Sect. B*, 2008, **266**, 3086–3090.
- 21 Y. P. Li and M. K. Lei, *J. Mater. Sci. Technol.*, 2014, **30**, 965–972.
- 22 J. Zimmermann, S. Seeger and F. A. Reifler, *Text. Res. J.*, 2009, **79**, 1565–1570.
- 23 P. N. Peszkin and J. M. Schultz, *J. Polym. Sci., Part B: Polym. Phys.*, 1986, **24**, 2591–2616.
- 24 T. Murakami, S.-i. Kuroda and Z. Osawa, *J. Colloid Interface Sci.*, 1998, **202**, 37–44.
- 25 S. O. Kwon, C. H. Park and J. Kim, *J. Eng. Fibers Fabr.*, 2015, **10**, 46–56.
- 26 Y. Liu, J. H. Xin and C. H. Choi, *Langmuir*, 2012, **28**, 17426–17434.
- 27 G. Wua, T. Yoshidab and J. A. Cuculoc, *Polymers*, 1998, **39**, 6473–6482.
- 28 J. Yang, Z. Zhang, X. Xu, X. Zhu, X. Men and X. Zhou, *J. Mater. Chem.*, 2012, **22**, 2834.
- 29 I. Sas, R. E. Gorga, J. A. Joines and K. A. Thoney, *J. Polym. Sci., Part B: Polym. Phys.*, 2012, **50**, 824–845.

